Showing Different Images Simultaneously by using Chromatic Temporal Response in Human Vision

Hiroki Yamada, Fumihiko Sakaue and Jun Sato
Nagoya Institute of Technology, Nagoya 466-8555, Japan
{*yamada@cv., sakaue@, junsato@*}*nitech.ac.jp*

Keywords: Multiplex Image, Chromatic Response, Temporal Response, Human Retina.

Abstract: In this paper, we propose a novel method for showing different images to multiple observers simultaneously by using the difference in their chromatic and temporal retinal response. The chromatic and temporal response characteristics of human retina have individuality, and thus each observer observes slightly different image, even if the same image is presented to these observers. In this paper, we formalize the chromatic and temporal relationship between the input stimulus and the response in human vision, and propose a method for showing arbitrary different images to individual observers simultaneously by using the difference in chromatic temporal response characteristics. We also show a method for obtaining chromatic and temporal response of human vision. Experimental results from a special camera which reproduces the impulse response of human retina show that our proposed method can represent different and arbitrary images to multiple observers.

1 INTRODUCTION

In this paper, we consider multiplex image presentation, which enables us to show different images to multiple observers simultaneously by using a single display. If the multiplex image presentation is realized with a TV in a living room, multiple observers can watch different TV programs simultaneously by using a single TV set as shown in Fig.1. Also, if we use the multiplex image presentation on a vehicle display, the passengers can enjoy amusement programs on the display, while the driver uses the navigation system on the same display.

Recently Nonoyama et al. (Nonoyama et al., 2013) proposed a method for presenting different images to multiple observers by using the difference in spectral sensitivity characteristics of individual human vision. They showed that it is possible to encode multiple images into a single multi-band image, and decode these multiple images by using the spectral sensitivity characteristics of individual human vision. The method does not require any special glasses and does not have limitation in viewpoints and hence very efficient. However, since it encodes multiple images using small difference in spectral sensitivity of human vision, the images observed by multiple observers are not separated clearly if the color variations of multiple images are similar to each other or the spectral sensitivities of multiple observers are close to each other.

Figure 1: Multiplex image presentation. Multiple observers can enjoy different TV programs simultaneously by using a single display.

More recently, Ikeba et al (Ikeba et al., 2017) used the difference of the temporal response characteristics of individual human vision for solving the problem of chromatic similarity in multiple images and multiple observers. Although their method works well even if the objective images have similar color variations, observed images are not separated clearly if the temporal response characteristics of multiple observers are close to each other.

For solving these problems, we in this paper propose a multiplex image presentation method based on multiple response characteristics of human vision. In particular, we combine chromatic response characte-

Yamada, H., Sakaue, F. and Sato, J.
Showing Different Images Simultaneously by using Chromatic Temporal Response in Human Vision.
DOI: 10.5220/0007256700670074
In *Proceedings of the 14th International Joint Conference on Computer Vision, Imaging and Computer Graphics Theory and Applications (VISIGRAPP 2019)*, pages 67-74
ISBN: 978-989-758-354-4

ristics with temporal response characteristics in human vision for separating observed images more clearly. By combining multiple characteristics in human vision, we show that different images can be observed by multiple observers, even if the color variations of objective images are similar to each other, and even if one characteristic in human vision is identical among multiple observers.

2 RELATED WORK

The multiplex image presentation enables us to show multiple different images to individual observers (Hamada et al., 2010; Kakehi et al., 2005; Nonoyama et al., 2013; Muramatsu et al., 2016; Ikeba et al., 2017). It is often used for displaying 3D images to human observers, in which left and right eyes of the observer observe different images.

Unfortunately, the existing multiplex image presentation methods require special equipments, such as stereo glasses for separating a single multiplex image into multiple images. The parallax barriers (Berthier, 1896; Ives, 1902) and lenticular lenses (Lippmann, 1908) are also used for separating multiplex images according to the viewpoint of observers. However, the position of the viewpoint is fixed in these methods, and thus observers cannot observe objective images at arbitrary viewpoints. For moving observers, Perlin et al. (Perlin et al., 2000) proposed a method, which controls light rays of the display according to the viewpoint of the observer, so that the observer can see appropriate images at any viewpoint. More recently, complex light field displays were developed and used for showing dense light fields toward multiple observers simultaneously (Masia et al., 2013; Wetzstein et al., 2011; Wetzstein et al., 2012; Hirsch et al., 2014; Lanman and Luebke, 2013; Huang et al., 2015). These methods are very useful when we want to display same 3D information to all the observers. However, if we want to display different images to individual observers regardless of their viewpoints, these existing methods fail, since all these methods are based on the geometric difference of viewpoints.

Recently, Nonoyama et al.(Nonoyama et al., 2013) proposed a new method for displaying multiplex images without using the geometric properties of light fields. In their method, they used not the characteristics of equipments, but the characteristics of human observers for displaying different images to individual observers. In particular, they used the difference of spectral sensitivity of human vision for displaying different images to individual observers. Their method does not require special glasses nor the

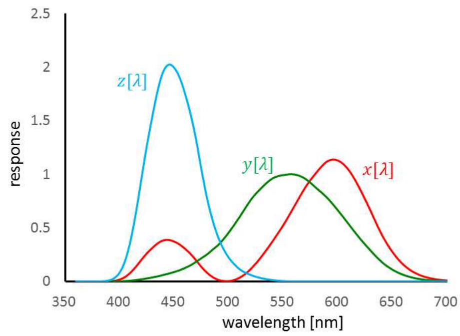

Figure 2: Color matching functions defined by CIE (CIE, 1931), which describe the spectral sensitivity of a standard human observer.

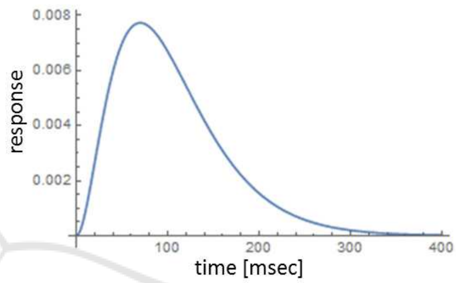

Figure 3: Impulse response of human vision.

fixation of viewpoints. However, it cannot be used when the spectral sensitivities of observers are similar to each other or objective images of multiple observers have similar color variation.

In order to overcome these problems, Ikeba et al. (Ikeba et al., 2017) proposed a method for displaying multiplex images by using the temporal response characteristics of human vision. In their method, the difference in the reaction time of human retina was used for presenting different images to multiple observers.

Unfortunately, these methods fail to present clearly separated images to individual observers. Thus, we in this paper combine multiple response characteristics of human observers. In particular, we combine chromatic response characteristics and temporal response characteristics of human vision, and realize better separation of observed images.

3 CHROMATIC TEMPORAL RESPONSE OF VISION

We first consider the chromatic and temporal response characteristics of human vision. The chromatic response of human vision can be characterized by the spectral sensitivity of 3 different photoreceptor cells in human retina, that is L-cone , M-cone and S-cone.

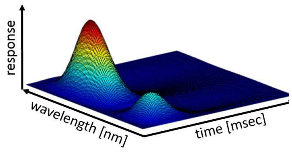

(a) $H_x(\lambda,t)$

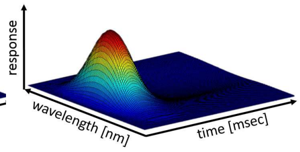

(b) $H_y(\lambda,t)$

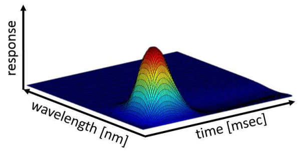

(c) $H_z(\lambda,t)$

Figure 4: Chromatic temporal response function of human vision.

These three cone cells are sensitive to long wavelength light, medium wavelength light and short wavelength light respectively.

The color perception caused by these 3 cone cells can be associated with physical light spectra by using the color matching functions, $x(\lambda)$, $y(\lambda)$ and $z(\lambda)$, whose spectral distributions are as shown in Fig. 2. These 3 color matching functions can be considered as the spectral sensitivity of a standard human observer in 3 channels. Thus, we in this paper consider the individuality in chromatic response of human vision as the individuality in color matching functions, $x(\lambda)$, $y(\lambda)$ and $z(\lambda)$.

On the other hand, the temporal response of human vision is described by the temporal impulse response of photoreceptor cells, that is the change in response in time when the light impulse is incident on a photoreceptor cell. It is known that the impulse response $S(t)$ of a typical photoreceptor cell can be described as shown in Fig. 3 (Cao et al., 2007).

It is known that the spectral sensitivity and the impulse response are different for every person (Cao et al., 2007). Thus, we consider a chromatic temporal response function $H(\lambda,t)$, which describes the chromatic and temporal response characteristics, for every person.

Since the chromatic temporal response function includes the spectral sensitivity characteristics and the temporal response characteristics, it is a two-dimensional function having response in two directions, i.e. wavelength direction and time direction, as shown in Fig. 4. Also, since it is considered that the spectral sensitivity characteristics and the temporal response characteristic are different for every channel, the chromatic temporal response function is defined for each channel $H_j(\lambda,t)$, $j \in \{x,y,z\}$ as shown in Fig. 4.

We next consider the observation model based on the chromatic temporal response function $H_j(\lambda,t)$. If

Figure 5: Multi-band projector.

we have an input light $E(\lambda,t)$ at time t, the observed intensity y^t_j of j-th channel at time t can be described as follows:

$$y^t_j = \int_{t-T}^{t} \int_{\lambda} H_j(\lambda, t-t')E(\lambda,t')d\lambda dt' \tag{1}$$

where, T is the observation period. We use the observation model in Eq.(1) for multiplex image presentation in the following part of this paper.

4 MULTIPLEX IMAGE PRESENTATION

4.1 Temporal Super-resolution of Multi-band Projector

In order to realize the multiplex image presentation, we in this paper control the spectral distribution and temporal change of incident light by using a high-speed multi-band projector.

Fig. 5 shows a multi-band projector composed of multiple projectors and narrow band-pass filters, and it can control the spectral distribution of projected light at each point on a screen. The incident light $E(\lambda,t)$ of the multi-band projector can be described by the spectral distribution $E_i(\lambda)$ of i-th band in the multi-band projector and its intensity p^t_i at time t as follows:

$$E(\lambda,t) = \sum_{i=1}^{N} E_i(\lambda)p^t_i \tag{2}$$

where, N is the number of bands in the multi-band projector.

By using such a multi-band projector, the observation model in Eq.(1) can be rewritten as follows:

$$y^t_j = \sum_{k=1}^{T}\sum_{i=1}^{N} h^j_{ki} p^{t-k+1}_i \tag{3}$$

where, h^j_{ki} is the response of j-th channel ($j \in \{x,y,z\}$) at discrete time k when the light impulse of i-th band

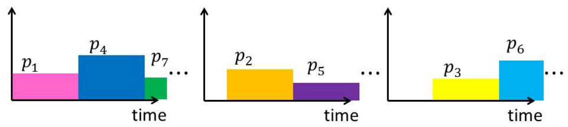

(a) switch timing is shifted in 3 projectors

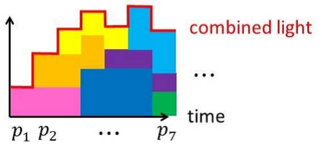

(b) temporal super resolution from 3 projectors

Figure 6: Temporal super resolution of projector.

is incident on the photoreceptor cell at time 0, and it is described by using the chromatic temporal response function $H_j(\lambda,t)$ and the spectral distribution $E_i(\lambda)$ of i-th band of the multi-band projector as follows:

$$h^j_{ki} = \int_{t-k}^{t-k+1} \int_\lambda H_j(\lambda, t-t')E_i(\lambda)d\lambda dt' \tag{4}$$

Furthermore, in order to control temporal response of human vision, a very fast light projection system is required. However, there is no high speed projector or display with high frame rate. Therefore, we consider temporal super resolution of projection systems by using multiple projectors whose timing of switching images is shifted to each other.

For example, if we have three projectors whose image switch timing is shifted with one third of the projection cycle as shown in Fig. 6 (a), then the intensity of image projected from these three projectors changes as shown in 6 (b). As a result, we can change images three times faster than the original projectors, and can achieve temporal super resolution of image projection. If we have K projectors for each band in the multi-band projector, the observation model of the high-speed multi-band projector can be described as follows:

$$y^t_j = \sum_{k=1}^{T}\sum_{i=1}^{N}\sum_{l=1}^{K} h^j_{ki} p_i^{t-k-l+2} \tag{5}$$

In this way, a high-speed multi-band projector can be realized.

4.2 Computing Projection Images for Multiplex Image Presentation

We next compute projection images for showing different images to different observers simultaneously using the high-speed multi-band projector.

Suppose we have M observers, and the chromatic temporal response functions $\{H^l_x(\lambda,t),\ H^l_y(\lambda,t),\ H^l_z(\lambda,t)\}$ $(l = 1,\cdots,M)$ of these M observers are

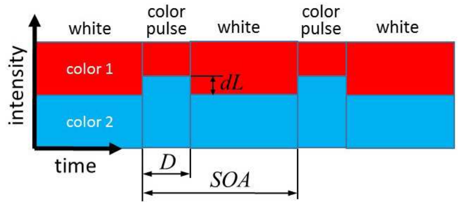

Figure 7: Temporal double-pulse method.

known. Then, the response function h^{jl}_{ki} of l-th observer can be computed from Eq.(4). Thus, given a set of sequential projection images p^t_i of the high-speed multi-band projector, the observation $y^{tl}_j(p^t_i)$ in j-th channel of the l-th observer at time t can be computed from Eq.(5).

Now, what we want to do is to show M different objective images $\hat{y}^{tl}_j$ $(l = 1,\cdots,M)$ to M observers. Thus, we estimate a set of sequential projection images p^t_i of the high-speed multi-band projector by solving the following minimization problem:

$$\{\hat{p}^t_i\} = \arg\min_{p^t_i} \sum_{l=1}^{M}\sum_{t=1}^{T}\sum_{j}^{\{x,y,z\}} (\hat{y}^{tl}_j - y^{tl}_j(p^t_i))^2 \tag{6}$$

However, since the projectors can only project images with a fixed range of intensity, the projection images p^t_i must hold the following inequality.

$$0 \le p^t_i \le I_{max} \tag{7}$$

where, I_{max} is the maximum intensity of projector light. Thus, we estimate the projection images p^t_i by solving Eq.(6) subject to Eq.(7). Then, the multiplex image presentation can be realized by presenting the image p^t_i from the high-speed multi-band projector toward these M observers.

5 MEASURING CHROMATIC TEMPORAL RESPONSE OF HUMAN VISION

We next consider a method for measuring chromatic temporal response function of human vision. For measuring the chromatic response characteristics, we use the existing method proposed by Muramatsu et al. (Muramatsu et al., 2016), which uses the metamerism in human color perception and estimate the spectral sensitivity of human vision efficiently.

For measuring the temporal response characteristics, we use the temporal double-pulse method proposed in the field of experimental psychology (Uchikawa and Yoshizawa, 1993). Since the temporal double-pulse method is not familiar in the computer vision field, we briefly explain the method.

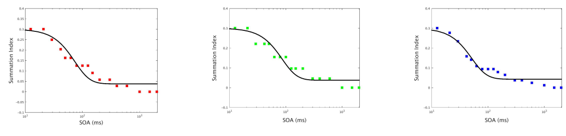

(a) summation index

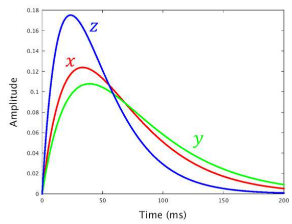

(b) impulse response

Figure 8: Summation index and estimated impulse response of human vision.

In this method, we show a white reference light and a sequential test light in the same field of view. The test light changes its color without changing its brightness by providing two color pulses as shown in Fig. 7, where dL is the amount of color in color pulse. If dL is small, the human vision cannot distinguish the test light from the white reference light, but if dL becomes large, the human vision can distinguish these two lights. So, we measure the threshold value of dL changing the test light.

In the test light, the length D of each pulse is fixed, but the interval of two color pulses is changed as shown in Fig. 7. The interval is called a stimulus-onset asynchrony (SOA). If SOA is large enough, two pulses are observed independently in the human vision, and double pulses and a single pulse dose not cause any difference in the observation. Therefore, the threshold value dL_d of the double pulse is same as the threshold value dL_s of the single pulse. However, when SOA becomes small, the impulse responses of double pulse overlap, and the photoreceptor has more excitation than that of the single pulse. As a result, dL_d becomes smaller than dL_s. Since the ratio of dL_d and dL_s changes according to the shape of the impulse response function, the impulse response function can be estimated from the ratio obtained by changing SOA. The ratio is called a summation index and is defined as follows:

$$SI = -\log\left(\frac{dL_d}{dL_s}\right) \tag{8}$$

If two impulse responses of the double pulse do not overlap, SI is equal to $-\log\frac{1}{1} = 0$, and if they overlap completely, SI is equal to $-\log\frac{1}{2} = 0.3$.

For estimating the impulse response function $S(t)$ efficiently, it is modeled by using two parameters, τ and n, as follows:

$$S(t) = \frac{1}{\tau^n(n-1)!}t^{n-1}e^{-\frac{t}{\tau}} \tag{9}$$

Thus, the estimation of $S(t)$ is considered as the estimation of τ and n.

Now, if we give some τ and n, then the impulse response $S(t)$ is fixed from Eq.(9) and the summation index $\hat{SI}(\tau,n)$ can be computed from Eq.(8). Therefore, we estimate τ and n, so that the computed summation index $\hat{SI}(\tau,n)$ becomes identical to the observed summation index SI. Thus, we estimate τ and n by solving the following minimization problem:

$$\{\hat{\tau},\hat{n}\} = \arg\min_{\{\tau,n\}} ||SI - \hat{SI}(\tau,n)||^2 \tag{10}$$

In this way, we can estimate the impulse response of an observer.

Then, by combining the spectral sensitivity and the impulse response, the chromatic temporal response function can be computed. In this research, it is assumed that the two characteristics are independent, and the chromatic temporal response function is described as the product of the spectral sensitivity characteristic $X(\lambda) \in \{x(\lambda), y(\lambda), z(\lambda)\}$ and the impulse response $S(t)$ as follows:

$$H(\lambda,t) = S(t)X(\lambda) \tag{11}$$

The estimated chromatic temporal response function can be used for realizing the multiplex image presentation described in section 4.

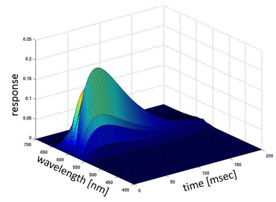

(a) x channel

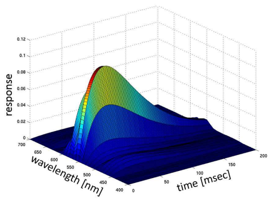

(b) y channel

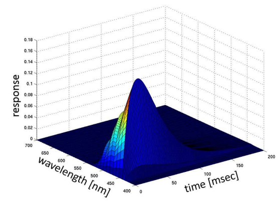

(c) z channel

Figure 9: Estimated chromatic temporal response functions.

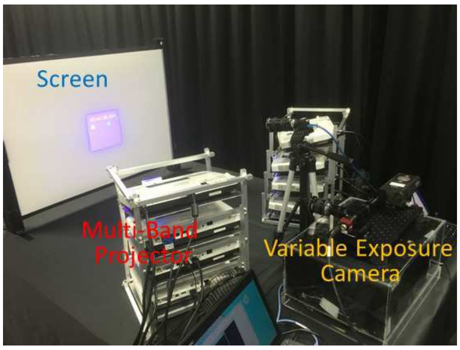

Figure 10: Experimental setup.

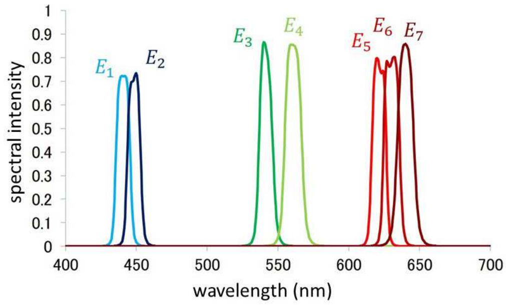

Figure 11: Spectral distribution of the multi-band (7-band) projector used in our experiments.

6 EXPERIMENTS

6.1 Estimation of Chromatic Temporal Response Function

We first show the results of chromatic temporal response estimation.

For measuring the summation index from the temporal double-pulse method, we used a high-speed display whose refresh rate is 240 fps. We changed the SOA of double pulse in the test light from 0 msec to 3000 msec, and measured the magnitude of color dL when the observer perceived the change in color.

Fig. 8 (a) shows the summation index of x, y and z channels estimated from the temporal double-pulse method. The points in the graph represent the summation index obtained from actual measurement, and the solid lines show the summation index computed from the parameters estimated by using these points.

Fig. 8 (b) shows impulse response of x, y and z channels estimated from the summation index in Fig. 8 (a).

By combining the spectral sensitivity estimated from the metamerism (Muramatsu et al., 2016), the chromatic temporal response functions were obtained as shown in Fig. 9.

6.2 Multiplex Image Presentation

We next show results of the proposed multiplex image presentation.

Since it is impossible to extract and show images observed by real human vision, we evaluated our multiplex image presentation by using a camera as an observer. Since the temporal response function of a standard camera cannot be controlled, we reproduced the chromatic temporal response function of human vision by using a variable exposure time camera proposed by Uda et al. (Uda et al., 2016), which can control the temporal exposure pattern freely in a single exposure time.

Our experimental setup is as shown in Fig. 10. The images are projected to the screen from the multi-band projector, and they are observed by the variable exposure time camera. The spectral distribution of the multi-band projector is as shown in Fig. 11. We reproduced two different chromatic temporal response functions, “observer A” and “observer B”, by using the variable exposure time camera.

Fig. 12 (a) shows objective images for these two observers, which we want to show them. As we can see in these images, the objective images for these two observers are completely different. From these objective image, we computed sequential projection images of the multi-band projector. The derived images were projected from the multi-band projector and observed by the variable exposure time camera. For comparison, we also implemented and tested two existing methods. The first one is a method proposed by Nonoyama (Nonoyama et al., 2013) which only uses the difference in spectral sensitivity, and the second one is a method proposed by Ikeba (Ikeba et al., 2017) which only uses the difference in temporal response.

Fig. 12 (b) shows images observed by observer A and B when we used the proposed method, and (c) and (d) show observed images in Nonoyama’s method and Ikeba’s method respectively. As we can see in these images, the proposed method enables us to show more clear and more independent images to these observers. The RMSE values also show that the proposed method provides us more accurate observation in multiplex image presentation.

Fig. 13 shows results from different objective images. As we can see in these results, our method works under various objective images.

We next evaluate the efficiency of the temporal super-resolution of projector in the multiplex image presentation. Fig. 14 shows the comparison of multiplex image presentation implemented by using high-speed projectors, temporal super-resolution of projectors and standard projectors. From these results,

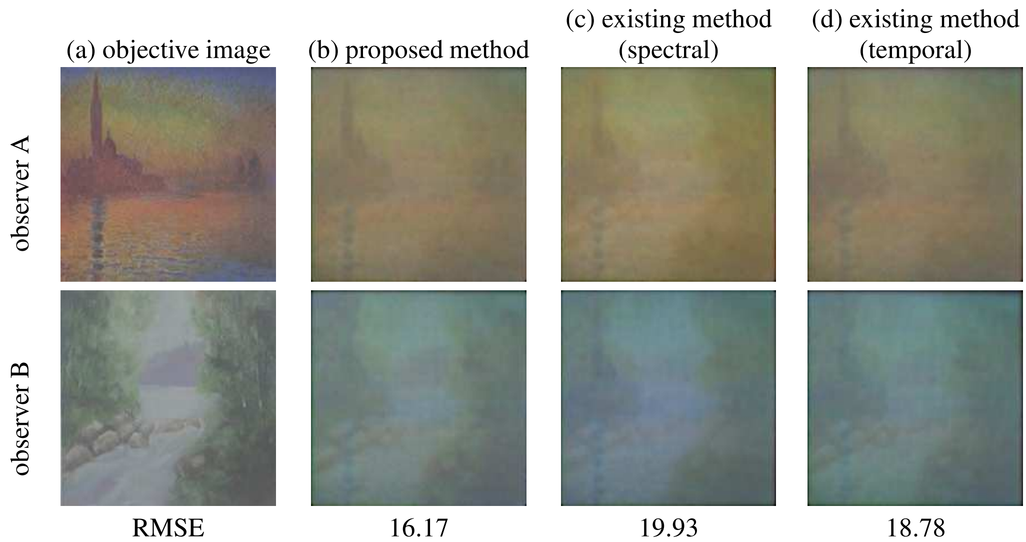

Figure 12: The results of multiplex image presentation.

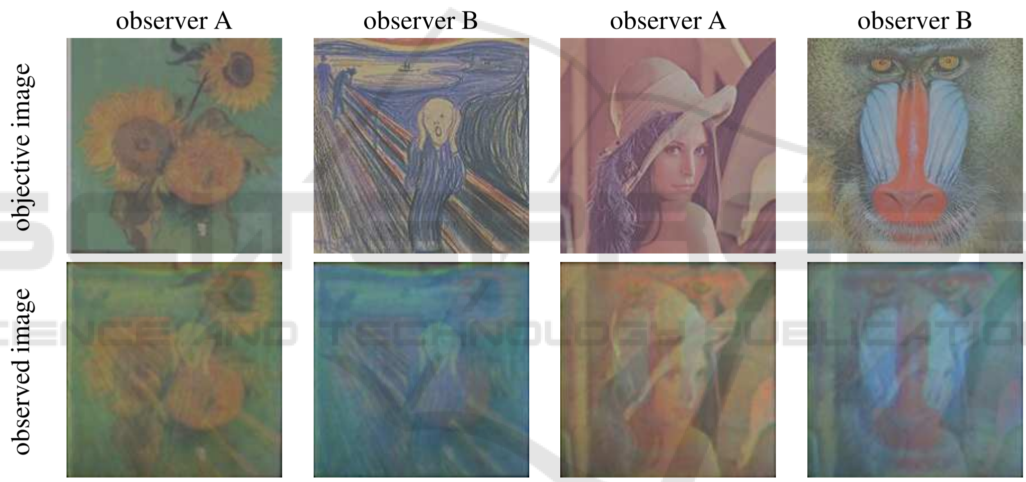

Figure 13: The results of multiplex image presentation (other results).

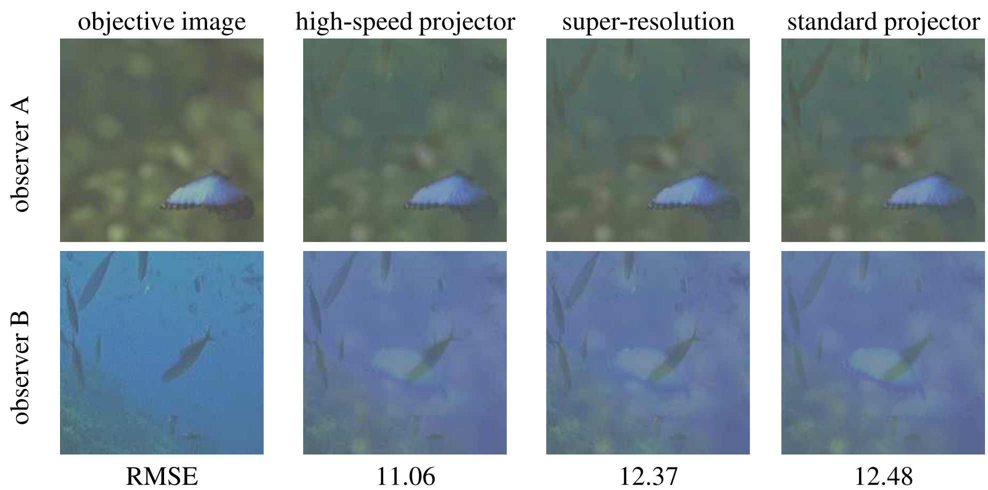

Figure 14: Comparison of multiplex image presentation from high speed projectors, temporal super-resolution of projectors and standard projectors.

we find that the temporal super-resolution provides us better quality in multiplex image presentation than the standard projectors.

7 CONCLUSION

In this paper, we proposed a novel method for showing different images to multiple observers simultaneously by using the difference in their chromatic and temporal retinal response.

We first formalized the chromatic and temporal relationship between the incident light and the response in human vision. Then, we proposed a method for showing arbitrary different images to individual observers simultaneously by using the difference in chromatic temporal response function in human vision. We also showed a method for obtaining the chromatic and temporal response function of human vision.

The experimental results show that the use of multiple visual response characteristics is efficient for realizing more accurate multiple image presentation.

REFERENCES

T. Hamada, K. Nagano and T. Scritters. A multiplexed image system for a public screen. In *Proc. Virtual Reality International Conference*. 321–323, 2010.

Y. Kakehi, M. Iida, T. Naemura, Y. Shirai, M. Matsushita and A. Ohguro. Lumisight table: An interactive view-dependent tabletop display. Computer Graphics and Applications, 25, 48–53, 2005.

M. Nonoyama, F. Sakaue and J. Sato. Multiplex image projection using multi-band projectors. In *Proc. IEEE Workshop on Color and Photometry in Computer Vision*, 2013.

K. Muramatsu, F. Sakaue and J. Sato. Estimating spectral sensitivity of human observer for multiplex image projection. In *Proc. International Conference on Computer Vision Theory and Applications*, 183–191, 2016.

D. Ikeba, F. Sakaue and J. Sato. Showing Different Images to Observers by using Difference in Retinal Impulse Response. In *Proc. International Conference on Image Analysis and Processing*, 718–729, 2017.

CIE. Commission internationale de l'Eclairage proceedings. Cambridge University Press, 1931.

D. Cao, A. Zele and J. Pokorny. Linking impulse response functions to reaction time. Vision Research, 47, 1060–1077, 2007.

A. Berthier. Images stereoscopiques de grand format. *Cosmos*, 34:205–210, 227–233, 1896.

F. Ives. A novel stereogram. *Journal of the Franklin Institute*, 153:51–52, 1902.

G. Lippmann. Epreuves reversibles donnant la sensation du relief. *Journal of Physics*, 7(4):821–825, 1908.

K. Perlin, S. Paxia and J.S. Kollin. An Autostereoscopic Display. In *ACM SIGGRAPH*, 2000.

B. Masiaa, G. Wetzsteinb, P. Didykc and D. Gutierrez. A survey on computational displays: Pushing the boundaries of optics, computation, and perception. Computer & Graphics, 37(8), 2012–1038, 2013.

G. Wetzstein, D. Lanman, W. Heidrich, and R. Raskar. Layered 3d: tomographic image synthesis for attenuation-based light field and high dynamic range displays. In *ACM Transactions on Graphics*, 30(4), 2011.

G. Wetzstein, D. Lanman, M. Hirsch, and R. Rasker. Tensor displays: Compressive light field synthesis using multilayer displays with directional backlighting. In *ACM Transactions on Graphics*, 2012.

M. Hirsch, G. Wetzstein, and R. Rasker. A compressive light field projection system. In *ACM Transactions on Graphics*, 2014.

D. Lanman and D. Luebke. Near-eye light field displays. In *ACM SIGGRAPH Asia*, 2013.

F. Huang, K. Chen, and G. Wetzstein. The light field stereoscope immersive computer graphics via factored near-eye light field displays with focus cues. In *ACM SIGGRAPH*, 2015.

Uchikawa, K., and Yoshizawa, T. Temporal Response to Chromatic and Achromatic Change Inferred from Temporal Double-Pulse Integration. *Journal of the Optical Society of America*, A, 1697–1705, 1993.

S. Uda, F. Sakaue and J. Sato. Variable exposure time imaging for obtaining hdr images. In *Proc. International Conference on Computer Vision Theory and Applications*, 118–124, 2016.